Odontology
https://doi.org/10.1007/s10266-026-01466-5

ORIGINAL ARTICLE

Mechanical and surface properties of resin-based materials for permanent use fabricated by subtractive, additive, and hybrid manufacturing techniques

Hande Gultekin[1] · **Zeynep Sahin**[1] · **Lale Karaagaclıoglu**[1]

Received: 9 March 2026 / Accepted: 1 June 2026
© The Author(s) 2026

Abstract

This in vitro study evaluated the flexural strength, elastic modulus, microhardness, and surface roughness of restorative materials fabricated using subtractive (SM, CAD/CAM milled control), additive (AM-DLP and AM-LCD), and hybrid (HM-LCD) manufacturing approaches. Grandio Disc was used as the reference baseline for the SM group, whereas VarseoSmile TriniQ was used for the AM and HM groups. Additive manufacturing groups included both DLP and LCD technologies to evaluate the influence of printing system. Standardized bar-shaped specimens (25 × 2 × 2 mm) were prepared according to ISO 4049:2019 for flexural testing, while disk-shaped specimens (15 mm in diameter × 1 mm in thickness) were used for Vickers microhardness measurements. Flexural strength, elastic modulus, and microhardness were measured, and surface roughness (Ra, Rz) was assessed. Manufacturing method significantly affected flexural strength, elastic modulus, and microhardness ($p < 0.001$), with the SM CAD/CAM control group exhibiting the highest values, followed by AM-LCD and AM-DLP, while the HM-LCD group showed the lowest values. Microhardness was highest in SM, with AM and HM groups showing similar values. Surface roughness (Ra) was higher in the additive groups (AM-DLP: 0.36 ± 0.07 µm; AM-LCD: 0.36 ± 0.01 µm) compared with the SM (0.27 ± 0.04 µm) and HM-LCD (0.29 ± 0.04 µm) groups. For Rz, the additive manufacturing groups showed higher values than the HM-LCD group ($p < 0.05$), whereas no significant differences were observed between the SM group and either the additive or hybrid groups. Both manufacturing method and material-related factors influenced the mechanical and surface properties of resin-based restorative materials. The SM group served as a clinically relevant reference baseline, while the inclusion of two different printing technologies allowed a comprehensive comparison of vat-photopolymerization systems.

Keywords Additive manufacturing · Hybrid manufacturing · Subtractive manufacturing · Mechanical properties · Surface roughness

Introduction

Computer-aided design and computer-aided manufacturing (CAD-CAM) systems integrate digital design and production processes and have significantly improved clinical efficiency by enhancing the precision and consistency of dental restorations [1]. The clinical integration of CAD-CAM technologies has made it possible to apply both subtractive (SM) and additive (AM) manufacturing approaches to the fabrication of restorative materials [2–4].

SM is considered a reliable prosthetic technique owing to its favorable esthetic outcomes, superior surface quality, and standardized manufacturing process [1–5]. Nevertheless, SM is associated with inherent limitations in design freedom, primarily due to restricted bur accessibility in complex geometries [6]. In contrast, AM has rapidly evolved and demonstrated considerable potential in dentistry by enabling the fabrication of complex structures, reducing material waste, and improving cost-effectiveness [1, 3, 6].

At present, additive manufacturing is supported by several technological platforms, most notably digital light

✉ Zeynep Sahin
zeynep.sahin@lokmanhekim.edu.tr

[1] Department of Prosthodontics, Faculty of Dentistry, Lokman Hekim University, Söğütözü. 2179 St, 06510 Çankaya, Ankara, Turkey

Published online: 15 June 2026

processing (DLP), stereolithography (SLA), and liquid crystal display (LCD)–based systems [4, 7, 8]. These technologies rely on different photopolymerization mechanisms and therefore exhibit distinct mechanical and surface characteristics [8]. Moreover, the properties of AM-fabricated restorations are influenced by multiple factors, such as layer thickness [9], build orientation [9, 10], and the type of printing material used [2].

Surface roughness is a critical parameter for restorative materials intended for permanent fixed prostheses, as increased roughness may promote plaque accumulation and bacterial adhesion [11]. Higher surface roughness promotes plaque retention and contributes to the development of dental caries as well as periodontal conditions such as gingivitis and periodontitis. For this reason, minimizing surface roughness is considered a clinically important objective [12–14]. The manufacturing precision of different fabrication techniques directly affects the ability to achieve optimal surface characteristics and mechanical performance [8, 15].

Hybrid manufacturing (HM) has emerged as a new production concept for dental restorations, in which AM and SM are brought together in a unified workflow [16]. In this approach, a resin block or ingot is first fabricated using AM, and the printed structure is subsequently milled using SM to achieve the final restoration geometry. This hybrid strategy combines the material efficiency and design flexibility of AM with the superior surface quality and dimensional precision of subtractive processing. This method involves milling resin ingots produced via AM using a subtractive workflow and has primarily been investigated for temporary restorations [16]. The HM approach aims to reduce manufacturing time and improve surface quality by minimizing the surface roughness typically associated with AM [17]. Although a limited number of studies have evaluated properties such as flexural strength, surface roughness, accuracy, precision, and internal fit of temporary crowns fabricated using HM [15, 17], no study has simultaneously assessed the mechanical and surface properties of permanent resin-based restorative materials produced using this approach.

With the development of digital manufacturing technologies, different restorative material classes have entered routine clinical practice through subtractive and additive workflows [1]. Because no resin composite is currently commercially available in a form compatible with both manufacturing techniques, a formulation-matched comparison is not attainable [18]. CAD/CAM-milled composites are generally characterized by a higher filler content and a more homogeneous microstructure, whereas additively manufactured resins undergo layer-by-layer photopolymerization, which may result in greater microstructural variability [19]. Although their chemical compositions are not identical, both material classes belong to resin-based composites containing an organic matrix and inorganic fillers and are widely used for definitive restorations [20]. Therefore, CAD/CAM-milled composite materials can be considered a clinically relevant reference baseline rather than a composition-matched control for comparison with additively manufactured resins. From this perspective, hybrid manufacturing may offer an additional conceptual advantage, because it allows additively manufactured resin to be further processed by milling, thereby creating a model in which surface and mechanical outcomes can be assessed within the same material background.

Based on these considerations, this in vitro study was designed to evaluate the flexural strength, elastic modulus, microhardness, and surface roughness of permanent resin-based restorative materials fabricated using subtractive, additive, and hybrid manufacturing workflows. Since the experimental groups reflected differences in both manufacturing approach and material composition, the findings were interpreted with consideration of both variables. It was hypothesized that the SM group would exhibit higher flexural strength, elastic modulus, and microhardness than the AM-DLP, AM-LCD and HM-LCD groups. In addition, comparable mechanical properties were expected among the AM-DLP, AM-LCD, and HM groups due to the use of the same resin system and identical post-curing conditions. It was further hypothesized that the HM group would demonstrate lower surface roughness than the AM groups due to the additional milling step.

Materials and methods

Power analysis and sample size determination

In this study, two different composite-based materials were selected and processed using SM, AM-DLP, AM-LCD and HM-LCD techniques (Table 1). A priori power analysis was performed using G*Power software (version 3.1.9.4; Heinrich Heine University Düsseldorf, Düsseldorf, Germany). The effect size was initially estimated based on previously published data from comparable studies, including Giugovaz et al. [17], which yielded very large values ($f \approx 1.70$ for flexural strength and $f \approx 0.76$ for surface roughness). However, these estimates were considered potentially inflated due to the limited sample size of the reference study and were not used for final sample size calculation. Therefore, a conservative large effect size ($f = 0.55$), in line with commonly reported values in dental materials research, was adopted for the final analysis (one-way ANOVA, fixed effects, $\alpha = 0.05$, power = 0.85, four groups). Based on this

Table 1 Materials used in the study, including their classifications, compositions, and manufacturers

Material	Classification	Composition	Manufacturer
Voco Grandio Disc	Nanohybrid composite processed via CAD/CAM milling	UDMA-based resin matrix; nanosilica (20–40 nm); barium–silicate glass fillers; pre-polymerized hybrid composite phase; filler content approximately 86 wt%	VOCO GmbH, Cuxhaven, Germany
VarseoSmile TriniQ	Additively manufactured microceramic hybrid composite resin	Esterification products of 4,4′-isopropylidenediphenol, ethoxylated and 2-methylprop-2-enoic acid; acrylate-based oligomeric matrix; benzeneacetic acid, alpha-oxo-, methyl ester; diphenyl(2,4,6 trimethylbenzoyl) phosphine oxide photoinitiator system	BEGO GmbH & Co. KG, Bremen, Germany

(UDMA: Urethane Dimethacrylate, wt%: Weight%)

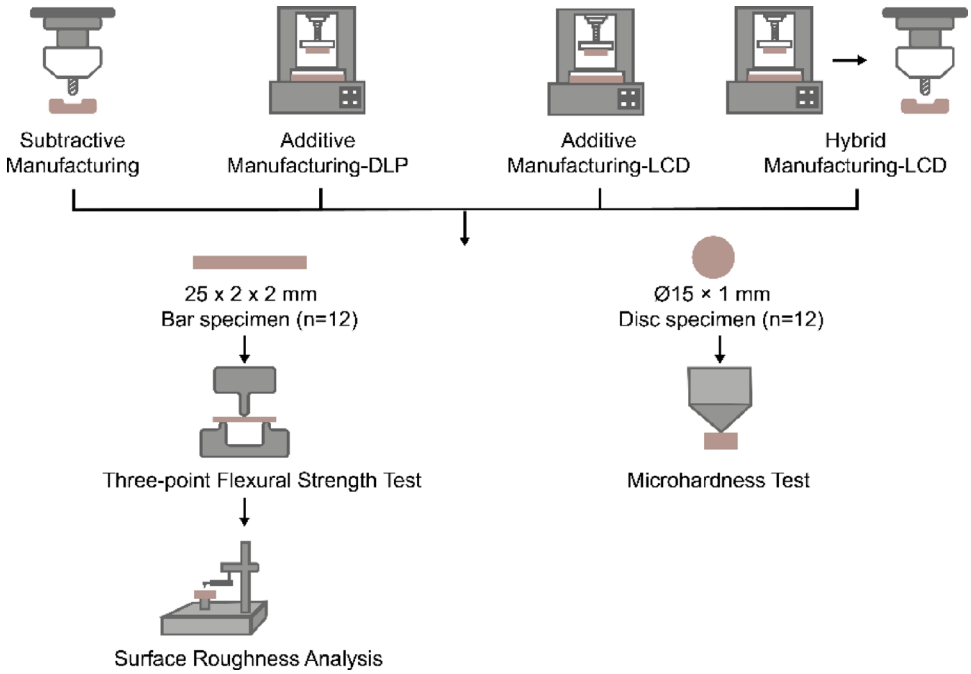


Fig. 1 Flowchart illustrating the sequential stages of specimen fabrication and mechanical and surface testing

analysis, a total of 48 specimens (12 per group) was determined to be sufficient, corresponding to an achieved power of 0.878.

Specimen design

Test specimens were fabricated in bar-shaped (25 × 2 × 2 mm) and disk-shaped (15 mm diameter × 1 mm thickness) geometries. Bar-shaped specimens were prepared in accordance with ISO 4049:2019 specifications [21], whereas disk-shaped specimens were prepared for Vickers microhardness testing. A total of 96 specimens were fabricated, comprising 12 bar-shaped and 12 disk-shaped specimens for each of the four experimental groups. Specimen geometries were designed using CAD software (SolidWorks 2024; Dassault Systèmes SolidWorks Corp, Waltham, Massachusetts, USA) and exported as standard tessellation language (.stl) files for digital manufacturing. The overall digital manufacturing workflow is illustrated in Fig. 1.

Specimen fabrication

To ensure methodological consistency and comparability across groups, both bar-shaped and disk-shaped specimens were fabricated within each experimental group using the same designated printing system and standardized workflow. Specimens in the SM group were fabricated from a nano-ceramic-filled resin-based composite disc material (Grandio Disc HT; VOCO GmbH, Cuxhaven, Germany) and milled using a computer-aided manufacturing (CAM) system (Redon GTR; Redon, Istanbul, Turkey).

Specimens in the AM-DLP group were fabricated using a DLP-based 3D printer with identical specifications (Asiga MAX; Asiga, Alexandria, Sydney, Australia) from a permanent composite resin-based material (VarseoSmile TriniQ; BEGO, Bremen, Germany). Printing was performed with a 50 µm layer thickness and 0° build orientation. After printing, specimens were ultrasonically cleaned in 96% ethanol for 5 min and air-dried. Post-curing was performed using a light-curing unit (Otoflash G171; NK Optik, Baierbrunn, Germany) with a spectral range of 300–700 nm (peak

emission 400–500 nm), delivering 4000 flashes (2 × 2000) at a flash frequency of 10 Hz under nitrogen atmosphere, according to the manufacturer's instructions.

Specimens in the AM-LCD group were fabricated using the same permanent composite resin-based material (VarseoSmile TriniQ; BEGO, Bremen, Germany) with an LCD-based 3D printer (Mars 5; ELEGOO, Shenzhen, China). The specimens were printed with a layer thickness of 50 µm and a build orientation of 0°. Post-processing procedures, including ultrasonic cleaning, air-drying, and post-curing, were performed using the same protocol applied to the AM-DLP group.

For the HM group, disc-shaped block (98 mm diameter × 15 mm thickness) was fabricated using the same permanent composite resin-based material (VarseoSmile TriniQ; BEGO, Bremen, Germany) with an LCD-based 3D printer (Mars 5; ELEGOO, Shenzhen, China). The printed blocks were produced with a layer thickness of 50 µm and a build orientation of 0°, and were subsequently milled to the final dimensions using the same CAM system (Redon GTR; Redon, Istanbul, Turkey) (Fig. 2). Post-processing procedures were performed using the same protocol applied to the AM-DLP group. This workflow is consistent with the HM approach described in the literature [16], and was implemented to maintain ISO compliance and specimen standardization across all groups.

Finishing and dimensional verification

After support removal, specimens across all groups underwent a stepwise polishing procedure using silicon carbide papers with grit levels of 600, 800, and 1200 to reduce surface irregularities. To verify dimensional accuracy, measurements were obtained from three different locations on each specimen using a digital caliper (Digital caliper 500-706-20; Mitutoyo, Kawasaki, Kanagawa, Japan), and mean values were recorded. All measurements were performed by a single calibrated examiner (G.H.) to ensure measurement consistency.

Flexural strength and elastic modulus testing

Bar-shaped specimens ($n = 12$ per group) were conditioned in distilled water at 37 ± 1 °C for 24 h in compliance with ISO 4049:2019, after which flexural testing was performed using a universal testing machine (Lloyd LRX; Lloyd

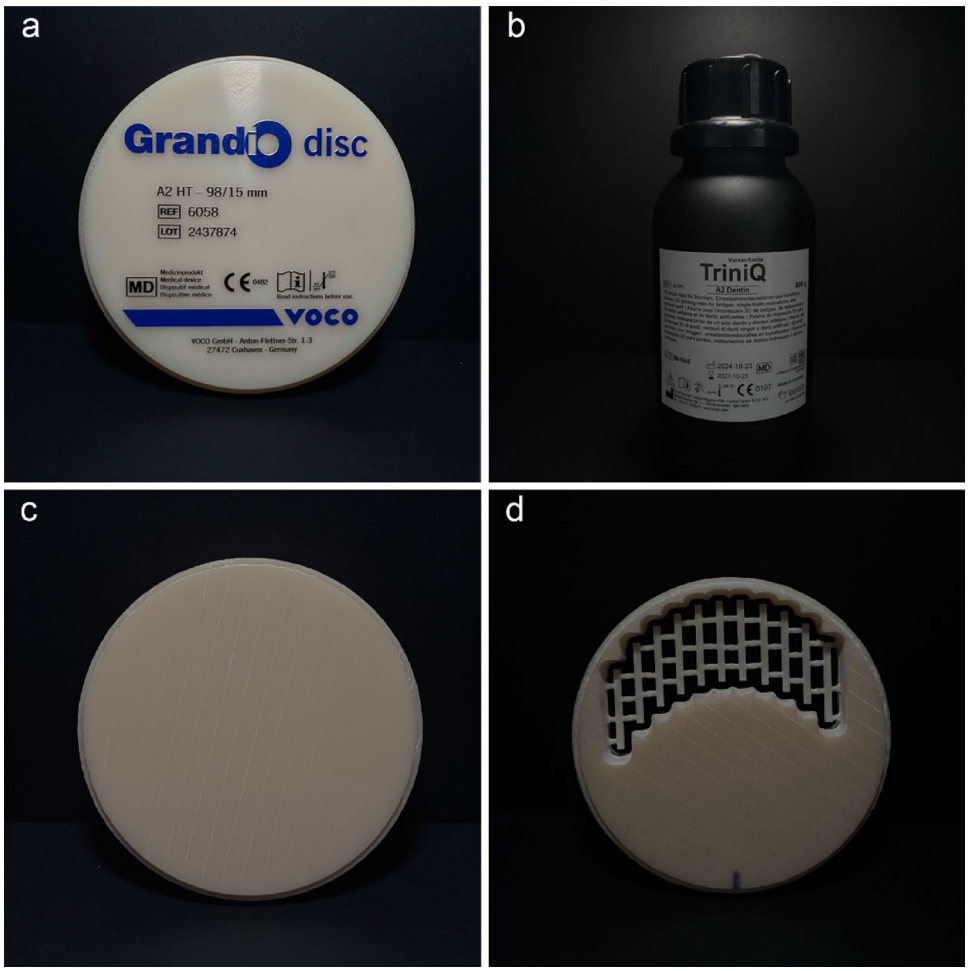


Fig. 2 Images of the materials and manufacturing processes used in the study. **a** Subtractive milling of a Voco Grandio disc. **b** Additive fabrication using permanent resin VarseoSmile TriniQ. **c** Initial step of the hybrid workflow: additive production of a VarseoSmile TriniQ disc. **d** Final step of the hybrid workflow: milling of the printed disc to obtain a bar

Instruments, Fareham, Hampshire, United Kingdom). Each specimen was placed on two supports with a 20-mm span and loaded at a crosshead speed of 1 mm/min until failure occurred. The maximum load at fracture was recorded and used to calculate flexural strength (σ) and elastic modulus (E) according to ISO 4049:2019, using the following equations:

$$\sigma = \frac{3FL}{2BH^2}$$

$$E = \frac{FL^3}{4BH^3d}$$

In these equations, F represents the maximum load at fracture, L denotes the support span length, B corresponds to the specimen width, H indicates the specimen thickness, and d represents the deflection measured in the linear region of the load–deflection curve.

Surface roughness measurements

After flexural testing, surface roughness parameters (Ra, Rz, and Rmax) were measured on the specimen surfaces using a contact profilometer (Perthometer; Mahr GmbH, Göttingen, Germany) ($n=12$). The evaluation length was set to 5.5 mm with a cutoff value of 0.8 mm, and the device was calibrated before each group measurement. For each specimen, three separate readings were recorded, and their average was taken as the representative value for statistical evaluation.

Microhardness testing

Disk-shaped specimens were evaluated for surface hardness using a microhardness tester (HVS-1000; AOB Lab, Shenzhen, China). Indentations were produced with a pyramidal diamond tip under a 4.9 N load applied for 15 s. Five separate impressions were created on each specimen, and their average was calculated and expressed as the Vickers hardness number (VHN).

Scanning electron microscopy (SEM) analysis

After completion of the mechanical tests, randomly selected specimens from each group were fixed onto aluminum stubs and coated with a gold–palladium layer by sputtering. Microstructural features and fracture-related patterns were subsequently analyzed by scanning electron microscopy (SEM) (SU-5000; Hitachi Ltd, Tokyo, Japan) operated at an accelerating voltage of 10 kV. Fracture surfaces were evaluated at magnifications ranging from ×45 to ×1000, whereas surface morphology was assessed at magnifications between ×1000 and ×10,000.

Statistical analysis

All statistical procedures were carried out with IBM SPSS Statistics software (version 29.0.1.0; IBM Corp, Armonk, New York, USA). Data normality was assessed through the Kolmogorov–Smirnov and Shapiro–Wilk tests, while homogeneity of variances was verified using the Levene test. Depending on distributional characteristics, intergroup differences were analyzed using one-way ANOVA for normally distributed variables or the Kruskal–Wallis test for non-normally distributed variables. Pairwise comparisons between independent groups were conducted using the Mann–Whitney U test. A p-value below 0.05 was considered indicative of statistical significance.

Results

Flexural strength, elastic modulus, and microhardness were measured to evaluate mechanical performance. Normality assessments showed deviations from a Gaussian distribution, leading to the use of nonparametric statistical methods. Statistically significant differences among the four groups were observed for all three parameters (Table 2).

Flexural strength

A statistically significant difference in flexural strength was observed among the groups (Kruskal–Wallis, $p<0.001$). Post hoc Mann–Whitney U tests revealed that the SM group showed the highest flexural strength, followed by the AM-LCD, AM-DLP, and HM-LCD groups. All pairwise comparisons were statistically significant ($p<0.05$).

Elastic modulus

The elastic modulus values also differed significantly (Kruskal–Wallis, $p<0.001$). The SM group had significantly higher elastic modulus values than the AM-DLP, AM-LCD, and HM-LCD groups ($p<0.05$). Additionally, no significant difference was observed between the AM-DLP and AM-LCD groups, whereas both groups had higher values than the HM-LCD group ($p<0.05$).

Microhardness

For microhardness, significant differences were detected among the groups (Kruskal–Wallis, $p<0.001$). The SM group showed higher microhardness than the AM-DLP,

Table 2 Flexural strength, elastic modulus, microhardness values of test specimens

Groups	Flexural strength (MPa)	Elastic modulus (GPa)	Microhardness (VHN)
	Mean ± SD / Median (IQR)	Mean ± SD / Median (IQR)	Mean ± SD / Median (IQR)
SM	205.59 ± 49.53 / 204.49 (79.82)[a]	14.60 ± 0.46 / 14.80 (0.35)[a]	122.59 ± 12.54 / 126.45 (19.59)[a]
AM-DLP	103.75 ± 14.81 / 98.34 (23.41)[b]	3.71 ± 1.11 / 3.37 (0.79)[b]	34.15 ± 5.83 / 33.31 (4.57)[b]
AM-LCD	119.25 ± 8.29 / 121 (12.58)[c]	3.62 ± 0.49 / 3.54 (0.66)[b]	33.76 ± 0.71 / 34 (1.06)[b]
HM-LCD	57.22 ± 13.75 / 52.72 (8.72)[d]	1.69 ± 0.65 / 1.61 (0.35)[c]	34.50 ± 1.22 / 34.12 (1.42)[b]
p value	**< 0.001**	**< 0.001**	**< 0.001**

Data are presented as mean ± standard deviation (SD) and median (interquartile range, IQR). Differences between groups were analyzed using the Kruskal–Wallis test and pairwise comparisons using the Mann–Whitney U test. Different superscripts (a-d) indicate statistically significant differences between groups ($p < 0.05$). SM, subtractive manufacturing; AM, additive manufacturing; HM, hybrid manufacturing; DLP, digital light processing; LCD, liquid crystal display

Table 3 Surface roughness values of test specimens

Groups	Ra (μm)	Rz (μm)	Rmax (μm)
	Mean ± SD / Median (IQR)	Mean ± SD / Median (IQR)	Mean ± SD / Median (IQR)
SM	0.27 ± 0.04[a] / 0.26 (0.06)	2.49 ± 0.33[a, b] / 2.41 (0.48)	3.26 ± 0.48 / 3.21 (0.76)[a]
AM-DLP	0.36 ± 0.07[b] / 0.34 (0.15)	2.63 ± 0.46[a] / 2.57 (0.71)	3.37 ± 0.70 / 3.09 (0.90)[a]
AM-LCD	0.36 ± 0.01[b] / 0.37 (0.03)	2.51 ± 0.13[a] / 2.54 (0.14)	3.42 ± 0.18 / 3.43 (0.32)[a]
HM-LCD	0.29 ± 0.04[a] / 0.27 (0.07)	2.14 ± 0.26[b] / 2.18 (0.42)	2.96 ± 0.49 / 3.06 (0.77)[a]
p value	**< 0.05**	**< 0.05**	0.345

Surface roughness parameters were analyzed using one-way ANOVA with Tamhane T2 post-hoc test for Ra, ANOVA with Tukey HSD for Rz, and the Kruskal–Wallis test for Rmax. Groups sharing at least one common superscript letter are not significantly different, whereas groups with no common superscript letters differ significantly ($p < 0.05$). SM, subtractive manufacturing; AM, additive manufacturing; HM, hybrid manufacturing; DLP, digital light processing; LCD, liquid crystal display

AM-LCD, and HM-LCD groups ($p < 0.05$). However, no significant difference was observed between the AM-DLP, AM-LCD, and HM-LCD groups ($p > 0.05$) (Table 2).

Surface roughness

Surface roughness outcomes varied across the experimental groups. Ra values were significantly greater in the AM-DLP and AM-LCD groups compared with the SM and HM-LCD groups ($p < 0.05$), whereas no significant difference was observed between the SM and HM-LCD groups or between the AM-DLP and AM-LCD groups. For Rz, the HM-LCD group showed lower values than the AM-DLP group ($p < 0.05$), while the comparisons involving the SM and AM-LCD groups did not reach statistical significance. In contrast, Rmax values did not differ significantly among the groups ($p = 0.345$) (Table 3).

Scanning electron microscopy (SEM) analysis

Representative SEM images revealed differences in surface morphology among the groups (Fig. 3). The SM group exhibited a more uniform surface morphology with finer topographical features (Fig. 3a-d). The AM-DLP and AM-LCD groups displayed more pronounced surface irregularities (Fig. 3e–l), whereas the HM-LCD group showed relatively smoother surface characteristics compared with the AM groups (Fig. 3m–p). These observations were qualitative in nature, and no interpretation regarding material composition was made.

In all groups, fracture initiation was identified at the surface region subjected to tensile stress. Fractographic analysis revealed characteristic brittle fracture features, including a well-defined fracture origin, a mirror region, mist–hackle patterns, and compression curl features developing toward the final stage of crack propagation (Fig. 4). In the AM-DLP and AM-LCD groups, the mirror, mist–hackle, and compression curl regions were clearly distinguishable, and the fracture surfaces exhibited faceted, sharp-edged features, allowing crack propagation paths to be readily identified (Fig. 4d and g). A more uniform fracture surface morphology with less pronounced fracture features was observed in the SM specimens (Fig. 4a). In contrast, the HM-LCD group exhibited fracture lines that were less clearly defined than those seen in the other groups (Fig. 4j).

Discussion

In the present in vitro study, the mechanical and surface properties of permanent resin-based restorative materials fabricated using four different digital manufacturing workflows were compared. The findings showed that the material–manufacturing workflow influenced both mechanical performance and surface roughness. The HM-LCD group exhibited more favorable surface characteristics, with Ra

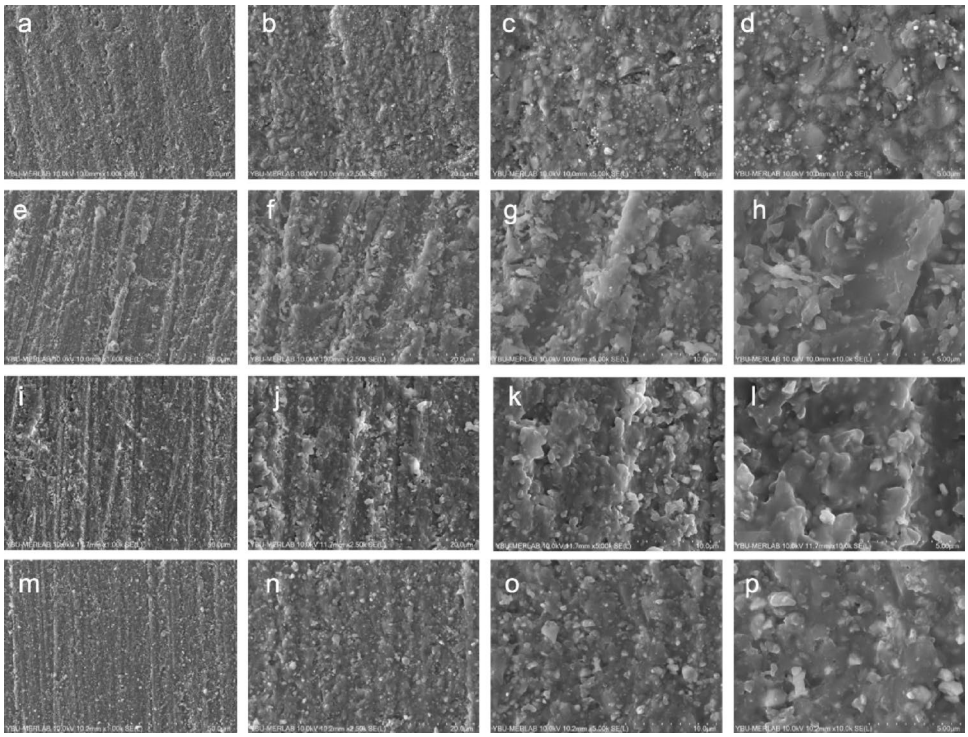


Fig. 3 SEM images showing the surface morphology of specimens fabricated using different digital manufacturing techniques: subtractive manufacturing (SM; **a**–**d**), additive manufacturing by DLP (AM-DLP; **e**–**h**), additive manufacturing by LCD (AM-LCD; **i**–**l**), and hybrid manufacturing by LCD (HM-LCD; **m**–**p**). Images were obtained at ×1000, ×2500, ×5000, and ×10,000 magnifications from left to right

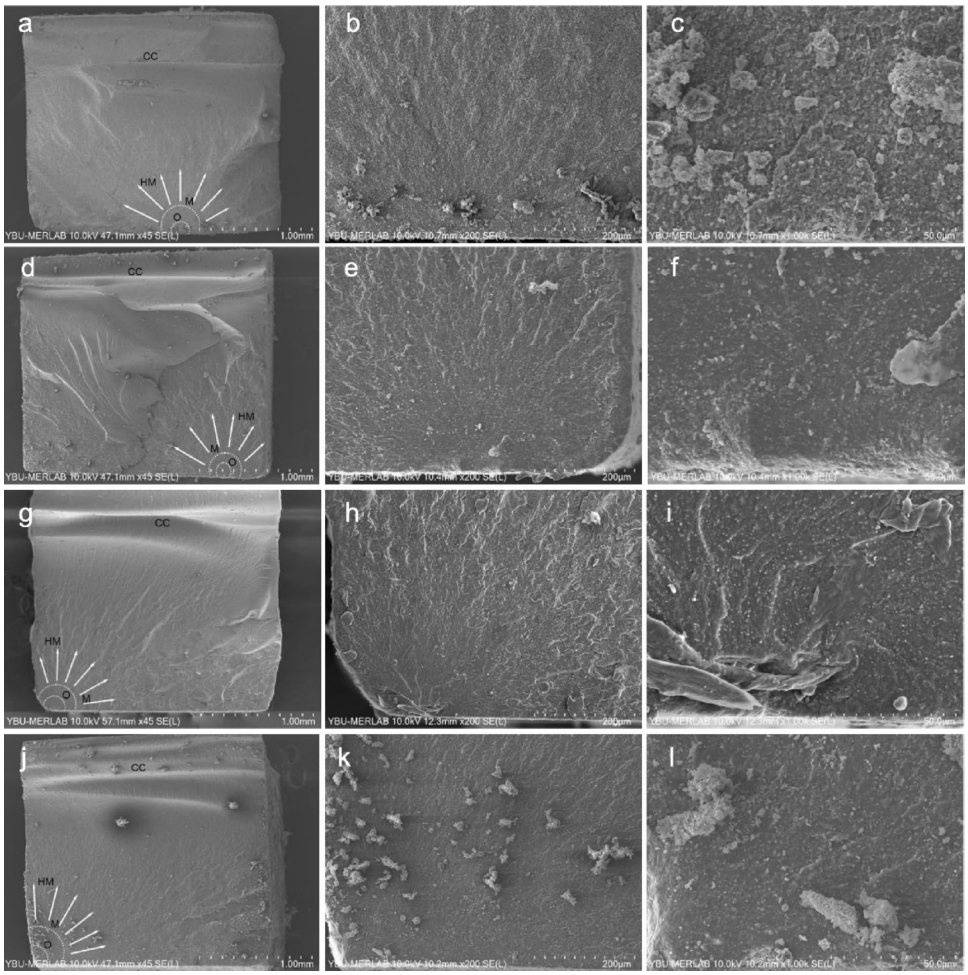


Fig. 4 SEM images showing the fracture surface characteristics of test specimens manufactured using different digital manufacturing techniques. Images **a**–**c** represent the subtractive manufacturing (SM) group, **d**–**f** the additive manufacturing (AM-DLP) group, **g**–**i** the additive manufacturing (AM-LCD) group and **j**–**l** the hybrid manufacturing (HM-LCD) group. Images a, d, g and j (×45) illustrate the fracture origin (O), mirror region (M), wake hackle markings (HM), direction of crack propagation (white arrows), and compression curl (CC). Images b, e, h and k (×200) present close-up views of the fracture origin (O), mirror region (M), and hackle markings (HM), while images c, f, i and l (×1000) show detailed views of the fracture origin

and Rz values comparable to those of the SM group and lower than those of the AM-DLP and AM-LCD groups. However, this surface advantage was accompanied by the lowest flexural strength and elastic modulus values. Microhardness was similar among the AM-DLP, AM-LCD, and HM-LCD groups, whereas the SM group consistently showed the highest mechanical performance. Therefore, the study hypotheses were only partially confirmed: although the HM group demonstrated lower surface roughness than the AM groups, the expectation that the AM-DLP, AM-LCD, and HM-LCD groups would show comparable mechanical properties was not supported.

The SM group was fabricated from Grandio Disc, a high filler-content CAD/CAM composite commonly used as a control material in SM studies [19, 22], whereas the AM-DLP, AM-LCD and HM-LCD groups were produced using VarseoSmile TriniQ, a resin specifically formulated for additive manufacturing. Similar to previous investigations comparing subtractive and additive fabrication methods, the use of identical material compositions across all groups was not feasible due to the limited availability of materials compatible with both techniques. In many such studies, milled materials are employed as control groups despite differences in chemical formulation [17, 23].

Fractures in permanent restorations represent one of the leading causes of clinical failure [24]. Within this context, flexural strength is a key mechanical parameter for polymer-based restorative materials and is assessed according to the ISO 4049:2019 standard [21]. In the present study, the SM group exhibited significantly higher flexural strength than the AM-DLP, AM-LCD, and HM-LCD groups, a finding that is consistent with previous reports comparing milled and additively manufactured resin-based materials [2, 17, 22, 25]. However, this difference should not be attributed solely to the manufacturing technique.

This difference may be explained by the higher filler content of the SM material, which is reported to be approximately 86% [13]. Prause et al. demonstrated that SM-fabricated resin materials present a more homogeneous microstructure, smaller filler particle sizes, and a higher filler ratio compared with AM-DLP and AM-LCD specimens [26]. This observation is consistent with the SEM surface images of the present study. The reinforcing effect of high filler content is known to enhance mechanical performance by restricting polymer matrix deformation [2]. Therefore, the superior mechanical performance observed in the SM group may have been influenced not only by the subtractive manufacturing process but also by differences in material composition. Consequently, the mechanical outcomes should be interpreted by considering both the manufacturing technique and material-related variables. Variations between the flexural strength values obtained in this investigation and those reported by Grzebieluch et al. may therefore be attributed to differences in specimen dimensions as well as the post-curing protocol, particularly the use of continuous post-curing devices instead of photoflash systems [22, 27].

To date, limited evidence is available regarding the flexural strength of specimens fabricated using an HM approach that combines additive and subtractive techniques. Giugovaz et al. investigated the mechanical and surface properties of temporary resin materials produced using AM, SM, and HM methods and reported higher flexural strength values for HM specimens compared with those fabricated by AM [17]. The discrepancy between their findings and the outcomes obtained in this investigation can be partly explained by methodological differences, including the span length applied during three-point bending testing, which was set to 10 mm in their study and 20 mm in the current investigation. Furthermore, differences in the resin-based materials, 3D printing technologies, and milling systems employed limit the direct comparability of the reported outcomes.

According to ISO 4049:2019, resin-based restorative materials should exhibit a minimum flexural strength of 80 MPa [2, 21]. In the present study, this requirement was fulfilled by the SM, AM-DLP and AM-LCD groups, whereas the HM-LCD group did not reach the specified threshold. Standard bar specimens (25 × 2 × 2 mm) were manufactured in strict accordance with ISO 4049:2019. Two AM groups produced using different printing technologies, namely DLP and LCD, were evaluated in order to reflect the potential influence of printer type on mechanical behavior under the present experimental conditions. Variations in polymerization behavior and mechanical performance have been reported between different 3D printing technologies, including DLP and LCD systems [28]. In both DLP and LCD technologies, the polymerization of each cross-sectional layer occurs in a single exposure; however, differences in light intensity distribution and potential light leakage in LCD systems may lead to variations in the degree of conversion across layers [4, 8]. Although LCD-based printing offers advantages such as lower cost and reduced geometric distortion, light diffusion through the liquid crystal panel may adversely affect mechanical properties [4, 7]. Within this framework, the fabrication workflow may influence the polymerization behavior and mechanical performance of additively manufactured materials. The fact that the AM-LCD group exceeded the ISO threshold, whereas the HM-LCD group did not, suggests that the reduced flexural strength in the HM-LCD group cannot be attributed to LCD-based printing alone. It may also be related to limited post-curing efficiency within the printed resin structure, possibly due to the larger printed block geometry used in the HM workflow. Post-polymerization is essential for

achieving the optimal physical properties of vat-photopolymerized materials, and the degree of polymerization is known to significantly influence the mechanical behavior of resin-based restorative materials [29–31]. Similarly, Kim et al. reported lower flexural strength in thicker resin specimens after post-polymerization, suggesting that reduced light transmission with increasing thickness may adversely affect the final physical properties and may require longer curing time or higher light intensity to compensate for light attenuation. Because increased thickness may restrict light penetration, reduce conversion in deeper regions, and compromise cross-linking, the printed block size used in the HM workflow may have contributed to inferior mechanical performance [29, 32]. In addition, the subsequent milling step may have further weakened the material by introducing surface defects or microcracks, as previously suggested for resin-based CAD/CAM materials [23]. These defects may act as stress concentrators and potentially initiate fatigue-related failure under loading conditions. Therefore, the low flexural strength observed in the HM-LCD group may plausibly reflect the combined influence of incomplete polymerization and milling-induced structural damage rather than a single factor alone. From a clinical standpoint, the SM, AM-DLP and AM-LCD approaches fulfilled the ISO 4049:2019 minimum flexural strength requirement and demonstrated more predictable mechanical performance under the conditions tested. In contrast, the HM-LCD group did not reach the 80 MPa threshold, which may indicate potential limitations, particularly in restorations subjected to higher occlusal loads [33]. However, because in vitro flexural strength values do not directly equate to clinical performance, the present findings should be interpreted cautiously when considering potential clinical applications.

When fracture patterns were examined, specimens in the SM, AM-DLP and AM-LCD groups exhibited typical brittle fracture behavior. However, in contrast to the AM group, SEM images of the SM specimens did not reveal distinct layer interfaces on the fracture surface, supporting a more homogeneous microstructure [2]. In the HM group, fracture surface images appeared relatively smoother and less defined compared with those of the SM and AM groups. This fracture morphology may reflect differences in crack propagation behavior and energy dissipation associated with the HM workflow [9].

While flexural strength is a fundamental parameter for comparing materials, it does not directly reflect material rigidity or deformation behavior under load. Therefore, the elastic modulus is a critical parameter for evaluating the stress–strain response of resin-based restorative materials [22, 34]. In the present study, the SM group exhibited elastic modulus values closest to those of natural dentin, which has been reported to range approximately between 16 and 29 GPa [34]. In a study by Mudhaffer et al. evaluating flexural strength and elastic modulus values of AM and SM specimens fabricated at different build orientations, the elastic modulus values reported for the AM groups were consistent with the findings of the current study, whereas lower values were reported for the SM group [2]. This discrepancy can be explained by variations in the material formulation, with specific reference to the lower filler proportion of the SM material used in the cited study compared with that employed in the current investigation. Reduced elastic modulus values have been associated with lower inorganic filler content and variations in filler particle morphology, both of which influence the stiffness of resin-based materials [35].

Vickers hardness reflects a material's resistance to localized plastic deformation under an applied indentation load [24]. In the present study, specimens produced using the SM method exhibited the highest microhardness values among the tested groups. Consistent with these findings, earlier investigations that evaluated additively and subtractively manufactured resin-based materials have demonstrated higher microhardness values for SM specimens [22, 36]. The similarity in surface microhardness values for the AM-DLP, AM-LCD and HM-LCD groups can be explained by the post-curing protocol that was applied. This finding is noteworthy because comparable microhardness values were observed despite the use of different printing technologies, suggesting that the identical post-curing protocol may have played an important role in surface hardness outcomes. Post-curing has been shown to significantly enhance microhardness by increasing the degree of polymer cross-linking and reducing residual monomer content [8]. In the present study, identical post-curing conditions were applied to all groups to minimize variability related to additional polymerization, which may explain the comparable microhardness values observed between the AM-DLP, AM-LCD and HM-LCD specimens. Nevertheless, the possible influence of printer-related polymerization characteristics should also be considered. LCD-based printing transmits light through a liquid crystal panel, which may affect light uniformity, irradiance, and exposure efficiency compared with DLP systems. These factors may influence polymerization behavior and, consequently, surface microhardness. However, previous studies comparing vat-photopolymerization technologies have reported similar surface hardness values among SLA, DLP, and LCD printed provisional restorative materials [8]. In agreement with these findings, no significant difference was observed between the AM-DLP and AM-LCD groups in the present study. Therefore, under standardized post-curing conditions, printing technology alone may not have been a dominant determinant of microhardness outcomes.

The findings related to surface roughness, which represents one of the primary objectives of the HM approach,

were generally consistent with previous reports in the literature. Accordingly, lower surface roughness was recorded for the SM specimens relative to the AM specimens, consistent with findings from earlier studies [13, 14, 35]. In the present study, the HM-LCD group also demonstrated improved surface characteristics, with Ra values comparable to those of the SM group and lower than those of the AM-DLP and AM-LCD groups. A similar trend was observed for Rz, in which the HM-LCD group exhibited the lowest values among the tested groups. The quantitative Ra and Rz findings were consistent with the SEM observations, with the higher roughness values of the AM-DLP and AM-LCD groups corresponding to more pronounced surface irregularities, whereas the lower roughness values of the HM-LCD group were associated with smoother surface characteristics that approached the more uniform morphology observed in the SM group. These findings suggest that the hybrid workflow may contribute to reducing the surface irregularities typically associated with additive manufacturing. However, unlike the surface roughness parameters, microhardness values were comparable among the AM-DLP, AM-LCD, and HM-LCD groups, indicating that surface topography and surface hardness were not affected in the same manner under the present experimental conditions. To provide a more comprehensive assessment of surface topography, Rz and Rmax parameters were evaluated in addition to Ra [37]. Among restorative materials with similar Ra values, lower Rz and Rmax values are indicative of a smoother surface profile [38]. In the present study, Rz supported the Ra findings by favoring the HM-LCD group, whereas no statistically significant differences were detected among the groups with respect to Rmax.

Sassany et al. reported that a layer thickness of 50 µm resulted in the lowest Ra values in additively manufactured resin materials, which is consistent with the printing parameters applied in the present study [12]. In contrast, Giugovaz et al. observed lower surface roughness values for AM specimens and higher values for SM specimens when evaluating temporary restorative materials [17]. This discrepancy may be attributed to differences in material composition and polishability, as well as to the use of permanent resin materials in the present study [39]. The Ra values recorded in this study exceeded the commonly accepted 0.2 µm threshold for plaque retention [11, 12, 14]; however, these measurements represent post-fabrication surface conditions obtained after standardized abrasive finishing and without clinical polishing procedures. Therefore, they do not reflect the final intraoral surface characteristics of restorations. Considering that clinical polishing may substantially reduce surface roughness, the present findings should be interpreted cautiously in a clinical context and regarded as a comparison of material behavior under standardized laboratory conditions.

Qualitative evaluation of the SEM surface images revealed noticeable differences in surface morphology among the manufacturing methods. The AM-DLP and AM-LCD specimens exhibited more pronounced particulate features and a less uniform surface appearance, which may be associated with the layer-by-layer fabrication process inherent to additively manufactured polymers [19]. Although different printing technologies were used, both additive manufacturing groups showed generally similar surface morphological characteristics. In contrast, the SM specimens demonstrated a more homogeneous surface morphology with smoother transitions, consistent with their lower surface roughness values. The HM-LCD group showed an intermediate surface morphology, with reduced particle prominence compared with the AM-DLP and AM-LCD groups, while not fully reaching the homogeneity observed in the SM specimens. This observation suggests that the hybrid manufacturing approach may partially improve surface quality by combining additive fabrication with subtractive finishing procedures. However, as no quantitative analysis of particle size or distribution was performed, these interpretations should be regarded as qualitative observations.

HM approaches appear promising in mitigating the surface roughness–related limitations inherent to AM techniques. Nevertheless, further investigations are required to enhance their mechanical performance and to confirm their reliability for routine clinical use. This investigation was subject to several limitations, including the limited range of restorative materials, printing devices, and manufacturing technologies assessed. In addition, printing direction and layer thickness were not systematically varied. Although both DLP- and LCD-based vat-photopolymerization systems were incorporated into the study design, allowing comparison between additive manufacturing groups produced with different printing technologies, the hybrid manufacturing workflow could only be performed using the LCD-based system. During preliminary fabrication, DLP-printed specimens fractured during the milling stage; therefore, the HM group was fabricated using an LCD-based printer. To address this methodological issue, an additional AM-LCD group was included, which enabled comparison of DLP- and LCD-based additive manufacturing and provided a more direct comparison between AM-LCD and HM-LCD under the same printing technology. However, the absence of a DLP-based HM group remains a methodological limitation and should be considered when interpreting the mechanical outcomes. Further investigations are needed to explore the combined effects of various printing parameters and material systems across an expanded spectrum of additive and hybrid manufacturing platforms.

Conclusion

The mechanical and surface properties of the resin-based specimens varied according to the material–manufacturing workflow used. Under the conditions evaluated, SM demonstrated superior flexural strength, elastic modulus, and microhardness values. HM-LCD exhibited surface roughness values comparable to SM and lower than AM-DLP and AM-LCD; however, this surface improvement was accompanied by reduced overall mechanical performance, particularly lower flexural strength and elastic modulus values compared with both AM and SM groups.

These findings indicate that selecting a digital manufacturing strategy should balance mechanical requirements and surface quality. However, the potential influence of different vat-photopolymerization systems represents a methodological limitation, and the findings should be interpreted with caution. Further studies are needed to optimize hybrid manufacturing approaches and to clarify their clinical applicability.

Clinical implications

The observed differences among manufacturing approaches may be considered when selecting digitally fabricated resin-based restorations in situations requiring a balance between mechanical performance, including hardness, and surface quality, particularly in light of the lower surface roughness observed with the hybrid manufacturing approach compared with additive manufacturing.

Acknowledgements The authors thank BEGO GmbH & Co. KG for providing the materials used in this study.

Author contributions Conceptualization: Zeynep Şahin; Methodology: Hande Gültekin and Zeynep Şahin; Investigation: Hande Gültekin and Zeynep Şahin; Data curation: Hande Gültekin; Software: Hande Gültekin; Writing—original draft preparation: Hande Gültekin; Writing—review and editing: Zeynep Şahin and Lale Karaağaçlıoğlu; Supervision: Lale Karaağaçlıoğlu; Project administration: Hande Gültekin and Zeynep Şahin.

Funding Open access funding provided by the Scientific and Technological Research Council of Türkiye (TÜBİTAK). This research did not receive any funding.

Data availability The datasets generated and/or analyzed during the current study are available from the corresponding author upon reasonable request.

Declarations

Conflict of interest The authors declare no competing interests.

Ethical approval Ethical approval was not required for this study because it was conducted as an in vitro investigation.

Informed consent Nothing to declare.

Open Access This article is licensed under a Creative Commons Attribution 4.0 International License, which permits use, sharing, adaptation, distribution and reproduction in any medium or format, as long as you give appropriate credit to the original author(s) and the source, provide a link to the Creative Commons licence, and indicate if changes were made. The images or other third party material in this article are included in the article's Creative Commons licence, unless indicated otherwise in a credit line to the material. If material is not included in the article's Creative Commons licence and your intended use is not permitted by statutory regulation or exceeds the permitted use, you will need to obtain permission directly from the copyright holder. To view a copy of this licence, visit http://creativecommons.org/licenses/by/4.0/.

References

1. Németh A, Vitai V, Kelemen K, Teutsch B, Szabó B, Gerber G, et al. Comparison of fit and trueness of single-unit and short-span fixed dental restorations fabricated by additive and subtractive manufacturing—A systematic review and meta-analysis. J Dent. 2025;153:105527. https://doi.org/10.1016/j.jdent.2024.105527.
2. Mudhaffer S, Haider J, Satterthwaite J, Silikas N. Effects of print orientation and artificial aging on the flexural strength and flexural modulus of 3D printed restorative resin materials. J Prosthet Dent. 2025;133:1345–57. https://doi.org/10.1016/j.prosdent.2024.08.008.
3. Altinci P, Dönmez MB, Çakmak G, Al-Johani H, Kahveci Ç, Erkal D, et al. Additively manufactured resin-based endocrowns: Effect of material type, margin configuration, and pulp chamber depth on fabrication trueness and fit. J Dent. 2025;157:105731. https://doi.org/10.1016/j.jdent.2025.105731.
4. Lee H-E, Alauddin MS, Mohd Ghazali MI, Said Z, Mohamad Zol S. Effect of different vat polymerization techniques on mechanical and biological properties of 3D-printed denture base. Polymers. 2023;15:1463. https://doi.org/10.3390/polym15061463.
5. Çağlayan E, Sasany R, Bolat BN, Hartavi D, Batgerel O-E, Ucar SM, et al. Optical properties of repaired additively manufactured resin composites and zirconia and subtractively manufactured ceramics: A comparative study of composite resins. BMC Oral Health. 2025;25:144. https://doi.org/10.1186/s12903-025-05538-w.
6. Unkovskiy A, Diken Türksayar AA, Beuer F, Li P, Bomze D, Yassine J, et al. Influence of 3D-printed, milled and pressed lithium disilicate on the bond strength to two resin cements: An in vitro study. J Dent. 2025;157:105747. https://doi.org/10.1016/j.jdent.2025.105747.
7. Tsolakis IA, Papaioannou W, Papadopoulou E, Dalampira M, Tsolakis AI. Comparison in terms of accuracy between DLP and LCD printing technology for dental model printing. Dent J (Basel). 2022;10:181. https://doi.org/10.3390/dj10100181.
8. Katheng A, Prawatvatchara W, Chaiamornsup P, Sornsuwan T, Lekatana H, Palasuk J. Comparison of mechanical properties of different 3D printing technologies. Sci Rep. 2025;15:18998. https://doi.org/10.1038/s41598-025-03632-1.
9. Espinar C, Pérez MM, Pulgar R, Leon-Cecilla A, López-López MT, Bona AD. Influence of printing orientation on mechanical properties of aged 3D-printed restorative resins. Dent Mater. 2024;40:756–63. https://doi.org/10.1016/j.dental.2024.02.023.
10. Keßler A, Hickel R, Ilie N. In vitro investigation of the influence of printing direction on the flexural strength, flexural modulus and fractographic analysis of 3D-printed temporary materials. Dent Mater J. 2021;40:641–9. https://doi.org/10.4012/dmj.2020-147.

11. Kara D, Tekçe N, Fidan S, Demirci M, Tuncer S, Balcı S. The effects of various polishing procedures on surface topography of CAD/CAM resin restoratives. J Prosthodont. 2021;30:481–9. https://doi.org/10.1111/jopr.13278.
12. Sasany R, Jamjoon FZ, Kendirci MY, Yılmaz B. Effect of printing layer thickness on optical properties and surface roughness of 3D-printed resins: An in vitro study. Int J Prosthodont. 2024;37:165–73. https://doi.org/10.11607/ijp.8965.
13. Albrecht M, Schmidt F, Menzel F, Yassine J, Beuer F, Unkovskiy A. Comparative analysis of modern 3D-printed hybrid resin-ceramic materials for indirect restorations: An in vitro study. Polymers. 2024;16:3161. https://doi.org/10.3390/polym16223161.
14. Bataweel OO, Roulet J-F, Rocha MG, Zoidis P, Pereira P, Delgado AJ. Effect of simulated tooth brushing on surface roughness, gloss, and color stability of milled and printed permanent restorative materials. J Esthet Restor Dent. 2025;37:1773–83. https://doi.org/10.1111/jerd.13450.
15. Gamal N, El-Etreby A, Hamdy A, Taha D. Accuracy of resin-based crowns fabricated by a hybrid CAD-CAM manufacturing technique compared to subtractive and additive methods. J Esthet Restor Dent. 2025;37:1971–80. https://doi.org/10.1111/jerd.13448.
16. Pérez-Giugovaz MG, Mostafavi D, Revilla-León M. Additively manufactured ingot for interim dental restorations fabrication using a chairside milling machine. J Prosthodont. 2021;30:540–3. https://doi.org/10.1111/jopr.13349.
17. Giugovaz A, Pérez-Giugovaz MG, Al-Haj Husain N, Barmak AB, Özcan M, Revilla-León M. Flexural strength of aged and nonaged interim materials fabricated by using milling, additive manufacturing, and a combination of subtractive and additive methods. J Prosthet Dent. 2022;128:513e1. https://doi.org/10.1016/j.prosdent.2022.05.004.
18. Tayeb HK, Silikas N, Alhaddad AJ, Satterthwaite J. Flexural Strength and Hardness Analysis of 3D-Printed vs. Milled Resin Composites Indicated for Definitive Crowns. J Funct Biomater. 2025;16:468. https://doi.org/10.3390/jfb16120468.
19. Prause E, Malgaj T, Kocjan A, Beuer F, Hey J, Jevnikar P, et al. Mechanical properties of 3D-printed and milled composite resins for definitive restorations: An in vitro comparison of initial strength and fatigue behavior. J Esthet Restor Dent. 2023;36:391–401. https://doi.org/10.1111/jerd.13132.
20. Tribst JPM, Veerman A, Pereira GKR, Kleverlaan CJ, Dal Piva AMdO. Comparative strength study of indirect permanent restorations: 3d-printed, Milled, and Conventional Dental Composites. Clin Pract. 2024;14:1940–52. https://doi.org/10.3390/clinpract14050154.
21. International Organization for Standardization. Dentistry—Polymer-based restorative materials. ISO 4049. Geneva: ISO; 2019.
22. Grzebieluch W, Kowalewski P, Grygier D, Rutkowski-Gorczyca M, Kozakiewicz M, Jurczyszyn K. Printable and machinable dental restorative composites for CAD/CAM application—comparison of mechanical properties, fractographic, texture and fractal dimension analysis. Mater (Basel). 2021;14:4919. https://doi.org/10.3390/ma14174919.
23. Mandurino M, Cortili S, Coccoluto L, Greco K, Cantatore G, Gherlone EF, et al. Mechanical properties of 3D printed vs. subtractively manufactured composite resins for permanent restorations: A systematic review. Mater (Basel). 2025;18:985. https://doi.org/10.3390/ma18050985.
24. Borella PS, Alvares LAS, Ribeiro MTH, Moura GF, Soares CJ, Zancopé K, et al. Physical and mechanical properties of four 3D-printed resins at two different thick layers: An in vitro comparative study. Dent Mater. 2023;39:686–92. https://doi.org/10.1016/j.dental.2023.06.002.
25. Yılmaz D, Çakmak G, Güven ME, Pieralli S, Yoon H-I, Revilla-León M, et al. Effect of hydrothermal aging on the flexural strength and microhardness of materials used for additive or subtractive manufacturing of definitive restorations. Int J Prosthodont. 2024;37:133–41. https://doi.org/10.11607/ijp.8847.
26. Prause E, Hey J, Beuer F, Yassine J, Hesse B, Weitkamp T, et al. Microstructural investigation of hybrid CAD/CAM restorative dental materials by micro-CT and SEM. Dent Mater. 2024;40:930–40. https://doi.org/10.1016/j.dental.2024.04.006.
27. Li P, Lambart A-E, Stawarczyk B, Reymus M, Spintzyk S. Post-polymerization of a 3D-printed denture base polymer: Impact of post-curing methods on surface characteristics, flexural strength, and cytotoxicity. J Dent. 2021;115:103856. https://doi.org/10.1016/j.jdent.2021.103856.
28. Yıldırım Ö, Yeşil Z, Hatipoğlu Ö. Effect of different 3D-printing systems on the flexural strength of provisional fixed dental prostheses: A systematic review and network meta-analysis of in vitro studies. BMC Oral Health. 2025;25:82. https://doi.org/10.1186/s12903-025-05470-z.
29. Kim RJY, Kim D-E, Seo D-G. Post-polymerization of three-dimensional printing resin using a dental light curing unit. J Dent Sci. 2024;19:945–51. https://doi.org/10.1016/j.jds.2023.07.028.
30. Saini RS, Gurumurthy V, Quadri SA, Bavabeedu S, Abdelaziz KM, Okshah A, et al. The flexural strength of 3D-printed provisional restorations fabricated with different resins: a systematic review and meta-analysis. BMC Oral Health. 2024;24:66. https://doi.org/10.1186/s12903-023-03826-x.
31. de Paiva IRDV, Stabile VM, Alonso RCB, Puppin-Rontani RM, Correr-Sobrinho L, Correr AB. Simple post-curing methods to optimize the depth of cure and physicochemical properties of 3D printed resin. J Dent. 2025;158:105785. https://doi.org/10.1016/j.jdent.2025.105785.
32. Yay Kuscu HY, Gorus Z. Translucency, color, and hardness of 3D-printed provisional restorations. Sci Rep. 2025;15:27227. https://doi.org/10.1038/s41598-025-13020-4.
33. Martín-Ortega N, Sallorenzo A, Casajús J, Cervera A, Revilla-León M, Gómez-Polo M. Fracture resistance of additive manufactured and milled implant-supported interim crowns. J Prosthet Dent. 2022;127:267–74. https://doi.org/10.1016/j.prosdent.2020.11.017.
34. Ling L, Ma Y, Malyala R. A novel CAD/CAM resin composite block with high mechanical properties. Dent Mater. 2021;37:1150–5. https://doi.org/10.1016/j.dental.2021.03.006.
35. Di Fiore A, Stellini E, Alageel O, Alhotan A. Comparison of mechanical and surface properties of two 3D-printed composite resins for definitive restoration. J Prosthet Dent. 2024;132:45–55. https://doi.org/10.1016/j.prosdent.2024.07.003.
36. Çakmak G, Donmez MB, de Paula M, Akay C, Fonseca M, Kahveci Ç, et al. Surface roughness, optical properties, and microhardness of additively and subtractively manufactured CAD-CAM materials after brushing and coffee thermal cycling. J Prosthodont. 2025;34:68–77. https://doi.org/10.1111/jopr.13796.
37. Sahin Z, Ozer NE, Akan T, Kılıcarslan MA, Karaagaclıoglu L. The impact of different surface treatments on repair bond strength of conventionally, subtractive-, and additive-manufactured denture bases. J Esthet Restor Dent. 2024;36:1337–47. https://doi.org/10.1111/jerd.13248.
38. Ribeiro ABC, de Freitas RFCP, de Carvalho IHG, de Miranda LM, da Silva NR, de Fátima L Dantas de Almeida, et al. Flexural strength, surface roughness, micro-CT analysis, and microbiological adhesion of a 3D-printed temporary crown material. Clin Oral Investig. 2023;27:2207–20. https://doi.org/10.1007/s00784-023-04941-3.
39. Taşın S, Ismatullaev A, Usumez A. Comparison of surface roughness and color stainability of 3-dimensionally printed interim prosthodontic material with conventionally fabricated and

CAD-CAM milled materials. J Prosthet Dent. 2022;128:1094–101. https://doi.org/10.1016/j.prosdent.2021.01.027.

Publisher's Note Springer Nature remains neutral with regard to jurisdictional claims in published maps and institutional affiliations.